Coxiella burnetii Avoids Macrophage Phagocytosis by Interfering with Spatial Distribution of Complement Receptor 3[1]

Christian Capo,* Alix Moynault,* Yves Collette,† Daniel Olive,† Eric J. Brown,‡ Didier Raoult,* and Jean-Louis Mege[2]*

Phagocytosis is a highly localized event requiring the formation of spatially and temporally restricted signals. Numerous microorganisms have taken advantage of this property to invade host cells. *Coxiella burnetii*, the agent of Q fever, is an obligate intracellular bacterium that has developed a survival strategy in macrophages based on subversion of receptor-mediated phagocytosis. The uptake of *C. burnetii* is mediated by $\alpha_v\beta_3$ integrin and is restricted by impaired cross-talk of $\alpha_v\beta_3$ integrin and complement receptor 3 (CR3) (CD11b/CD18). In this study, we showed that CR3 molecules remained outside the pseudopodal extensions induced by *C. burnetii* in THP-1 monocytes, although $\alpha_v\beta_3$ integrin was present in the pseudopods. Chemoattractants such as RANTES restored CR3 localization to the front of pseudopodal extensions and increased *C. burnetii* phagocytosis, demonstrating that the localization of CR3 is critical for bacterial uptake. In addition, monocyte activation due to the expression of HIV-1 Nef protein also restored CR3-mediated phagocytosis of *C. burnetii* by allowing CR3 redistribution toward bacterial-induced pseudopods. The redistribution of CR3 and increased *C. burnetii* phagocytosis in THP-1 cells stimulated by RANTES or expressing Nef were associated with the inhibition of intracellular replication of *C. burnetii*. Hence, the localization of CR3 is critical for bacterial phagocytosis and also for the control of bacterial replication. This study describes a nonpreviously reported strategy of phagocytosis subversion by intracellular pathogens based on altered localization of monocyte receptors. ***The Journal of Immunology*****, 2003, 170: 4217–4225.**

Coxiella burnetii is an obligate intracellular microorganism classified in the γ subdivision of Proteobacteria (1). Its survival strategy in monocytes/macrophages is based on growth in acidic phagosomes that do not fuse with lysosomes (2). It is the etiologic agent of Q fever, a disease that typically manifests as an acute form in an immunocompetent host, and a chronic form in a host with defective cell-mediated immunity (3, 4). The entry of *C. burnetii* into human monocytes is a critical part of the infection. Although virulent *C. burnetii* organisms are poorly internalized, they survive in human monocytes. In contrast, avirulent organisms are more easily ingested than virulent organisms but fail to survive as intracellular pathogens. The uptake of avirulent *C. burnetii* is mediated by $\alpha_v\beta_3$ integrin and complement receptor 3 (CR3)[3] (CD11b/CD18), a β_2 integrin. Virulent organisms enter into monocytes through $\alpha_v\beta_3$ integrin and interfere with the activation of CR3 which appears to prevent efficient phagocytosis of bacteria (5). Hence, the impairment of CR3 function is a clue to an important virulence mechanism of *C. burnetii*.

To become competent for ligand binding and phagocytosis, CR3 must acquire an active configuration, which requires signals provided by other integrins, chemoattractant receptors, or LPS receptors (6). For example, the ligation of $\alpha_v\beta_3$ integrin and integrin-associated protein (IAP) enhances the binding efficiency of CR3 (7, 8). This is of particular relevance to *C. burnetii* infection because macrophages from $IAP^{-/-}$ knockout mice exhibit a profound decrease in CR3-mediated phagocytosis of avirulent *C. burnetii* (5). Although the mechanism of CR3 activation is incompletely understood, the capacity of CR3 to bind ligands efficiently is closely related to its aggregation state. For instance, CR3 clustering elicited by phorbol esters is correlated to increased binding and phagocytosis (9). The switch from an inactive to an active form is associated with an alteration in the mechanism of interaction of CR3 with the cytoskeleton (10). Although inactive CR3 molecules are linked to actin via talin, direct interaction of the β-chain of CR3 (CD18) with filamin and α-actinin occurs in phagocytic cells with activated integrins (11, 12). An immobile subset of CR3 linked to the cytoskeleton is more efficient for opsonic phagocytosis than freely diffusing receptors (13). The activation of β_2 integrins is also related to their diffusion rate and their release from cytoskeletal constraint (14, 15). Cytotoxic necrotizing factor-1 induces dramatic changes in F-actin organization, and impairs CR3 activity and its colocalization with F-actin in human monocytes (16). Together, these data implicate the monocyte cytoskeleton as a key regulator of CR3 function. We have reported that virulent, but not avirulent, *C. burnetii* organisms induce pseudopodal extensions and a profound reorganization of F-actin in THP-1 monocytes (17). For these reasons, we hypothesized that *C. burnetii*-mediated impairment of CR3 activity may result from effects on actin reorganization.

In this study, we showed that $\alpha_v\beta_3$ integrin, the *C. burnetii* receptor, was present on the pseudopodal extensions induced by virulent organisms in THP-1 monocytes. In contrast, CR3 molecules remained excluded from these protrusions. The spatial distribution

*Unité des Rickettsies, Faculté de Médecine, Centre National de la Recherche Scientifique Unité Mixte de Recherche 6020, Université de la Méditerranée, and †Institut National de la Santé et de la Recherche Médicale Unité 119, Institut Paoli-Calmettes, Marseille, France; and ‡Program in Microbial Pathogenesis and Host Defense, University of California, San Francisco, CA 94143

Received for publication July 11, 2002. Accepted for publication February 7, 2003.

The costs of publication of this article were defrayed in part by the payment of page charges. This article must therefore be hereby marked *advertisement* in accordance with 18 U.S.C. Section 1734 solely to indicate this fact.

[1] This work was supported by the Programme de Recherche en Microbiologie Fondamentale et Maladies Infectieuses et Parasitaires.

[2] Address correspondence and reprint requests to Dr. Jean-Louis Mege, Unité des Rickettsies, Faculté de Médecine, Center National de la Recherche Scientifique Unité Mixte de Recherche 6020, Université de la Méditerranée, 27 Boulevard Jean Moulin, 13385 Marseille Cedex 5, France. E-mail address: Jean-Louis.Mege@medecine.univ-mrs.fr

[3] Abbreviations used in this paper: CR3, complement receptor 3; IAP, integrin-associated protein; LPC, lysophosphatidylcholine; F-actin, filamentous actin.

0022-1767/03/$02.00

of CR3 is critical for the efficiency of *C. burnetii* phagocytosis. RANTES, a β-chemokine, induced pseudopodal extensions that expressed CR3 molecules, and up-regulated uptake of virulent *C. burnetii* through CR3-dependent mechanisms. The overexpression of HIV-1 Nef, known to stimulate macrophage activation, rescued CR3-mediated phagocytosis of *C. burnetii* via the redistribution of CR3 toward the pseudopodal extensions. The redistribution of CR3 in RANTES-stimulated THP-1 cells and in cells expressing Nef was associated with the prevention of *C. burnetii* replication. Our data suggest that the presence of CR3 at the leading edge of pseudopodal extensions is critical for *C. burnetii* uptake and for reprogramming the microbicidal process in macrophages. The disruption of this localization is likely a novel mechanism of immune escape by intracellular microorganisms.

Materials and Methods

Cells and bacteria

The human monocytic cell line THP-1 and the mouse fibroblast cell line L929 were obtained from the European Collection of Animal Cell Cultures (Sophia Antipolis, France). Circulating monocytes were isolated from PBMC, as previously described (5). THP-1 cells were cultured at 5×10^5 cells/ml in RPMI 1640 containing 20 mM HEPES, 10% heat-inactivated FCS, 2 mM L-glutamine, 100 U/ml penicillin, and 100 μg/ml streptomycin (Invitrogen, Eragny, France). THP-1 cells expressing Nef, an HIV-1 protein, were prepared as described elsewhere (18) and maintained in RPMI 1640 containing 10% FCS and 1 mg/ml neomycin (Invitrogen) to ensure continued selection of stably transfected cells. The expression of Nef was assessed by Western blot in cells cultured for 16 h in the presence or the absence of $CdCl_2$ (19). Total cell lysates were fractionated by SDS-PAGE followed by immunoblotting. Blots were revealed by chemiluminescence (Perkin-Elmer Life Sciences, Courtaboeuf, France).

C. burnetii (Nine Mile strain) was obtained as previously described (17). Virulent organisms (phase I organisms) were injected into mice and were recovered from spleen 10 days later. Spleen homogenates were added to L929 cell monolayers and cultures were maintained for two passages in antibiotic-free MEM supplemented with 4% FCS and 2 mM L-glutamine. Avirulent variants (phase II organisms) were obtained by repeated passages in L929 cells. Infected cells were sonicated, and sonicates were centrifuged at $300 \times g$ for 10 min to remove unbroken cells. Virulent and avirulent organisms were pelleted at $8000 \times g$ for 10 min, and purified on 25–45% linear Renografin gradient. Bacteria were aliquoted at 10^9 organisms/ml in HBSS and stored at −80°C.

Receptor distribution on individual monocytes

THP-1 monocytes (5×10^5 cells per assay) were stimulated with *C. burnetii* (bacterium-to-cell ratio of 100:1) or 10 ng/ml RANTES (R&D Systems, Abingdon, U.K.) in HBSS for 15 min at 37°C. In some experiments, they were preincubated with 10 μM PP1 (Alexis Biochemicals, Coger, France) or DMSO as vehicle 30 min before stimulation. Monocyte receptors were studied using large beads according to the technique of Wulfing and Davis (20). Some modifications were introduced to prevent bead uptake by monocytes. After stimulation, cells were washed and FcRs were saturated with PBS containing 1% BSA and 0.5% heat-inactivated horse serum (Invitrogen) for 30 min at 4°C. Monocytes were then incubated with mAbs directed against CD18 (1.5 μg), CD11b (3 μg), $\alpha_v\beta_3$ integrin (3 μg), IAP (3 μg), or control IgG1 for 30 min at 4°C in PBS containing 0.1% BSA. mAbs directed against CD11b (IgG1), CD18 (IgG1), and control IgG1 were purchased from Immunotech (Beckman-Coulter, Roissy, France). OKM1 mAb (IgG1) and BMS104 mAb (IgG1) directed against different domains of CD11b were from Ortho Diagnostic System (Roissy, France) and Bender Medsystems (Euromedex, Mundolsheim, France), respectively. The mAbs against IAP (2D3, IgG1) and $\alpha_v\beta_3$ integrin (7G2, IgG1) were generated as previously described (21). After washing, Dynabeads M-450 goat anti-mouse IgG (4.5-μm diameter; Dynal, Compiègne, France) at a 5:1 bead-to-cell ratio were added to monocytes for 15 min at room temperature under gentle shaking. In some experiments, Dynabeads M-280 sheep anti-mouse IgG (2.8-μm diameter; Dynal) were used instead of 4.5-μm beads. The study of cytoskeleton reorganization was studied as follows (17). Cell-bead complexes were fixed with 1% paraformaldehyde and incubated with PBS containing 10 U/ml bodipy phallacidin (Molecular Probes, Eugene, OR), and 100 μg/ml lysophosphatidylcholine (LPC; Sigma-Aldrich, St. Louis, MO) for 20 min. The localization of membrane-bound beads in pseudopodal extensions containing filamentous actin (F-actin) was determined with a laser scanning confocal fluorescence microscope (Leica, Lyon, France) equipped with a ×100 (NA 1.4) oil immersion lens. Serial optical sections of images were collected at 1-μm intervals along the *z*-axis using Scanware software, captured as TIFF files and analyzed with Adobe Photoshop 3.0 (Mountain View, CA). One hundred cells were examined per experimental condition. The results are expressed as the number of beads in and out of cell deformations and the percentage of beads in cell deformations.

In another set of experiments, THP-1 monocytes were stimulated by *C. burnetii* or RANTES and then incubated with specific mAbs. After washing, cells were incubated with a 1/50 dilution of FITC-conjugated $F(ab')_2$ anti-mouse IgG Abs (Immunotech) for 30 min at 4°C in the presence of Evans blue (Sigma-Aldrich). Cells were then washed and fixed with 1% paraformaldehyde. The localization of membrane receptors was determined by confocal microscopy, as described above.

Particle localization

THP-1 monocytes (5×10^5 cells per assay in RPMI 1640 with 20 mM HEPES) were incubated with avirulent *C. burnetii* (bacterium-to-cell ratio of 100:1), zymosan (1 mg/ml, Sigma Aldrich), or iC3b-coated E (E-to-cell ratio of 5:1) for 30 min at 20°C. iC3b-coated E was prepared as described elsewhere (22). Briefly, sheep E were coated with rabbit specific IgM and C5-deficient human serum (Sigma-Aldrich) in veronal-buffered saline containing dextrose, Ca^{2+} and Mg^{2+}. Monocytes were then washed to remove unbound particles. Bacteria were revealed by immunofluorescence. For that purpose, monocytes were fixed with 1% paraformaldehyde, and incubated with a 1/250 dilution of rabbit Abs specific for *C. burnetii*. After being washed, cells were incubated with a 1/200 dilution of FITC-conjugated $F(ab')_2$ anti-rabbit IgG (Immunotech). For the determination of zymosan localization, cell preparations were stained with DiffQuik (Baxter, Maurepas, France) before microscopic examination. The localization of iC3b-coated E was studied by light microscopy. More than 200 monocytes were counted in each assay. Results are expressed as the percentage of bacteria or particles present in cell deformations.

Phagocytosis assay

THP-1 monocytes (5×10^5 cells per assay in RPMI 1640 containing 20 mM HEPES and 10% heat-inactivated FCS) were incubated with zymosan (1 mg/ml), iC3b-coated E or IgG-coated E (E-to-cell ratio of 20:1) for 1 h at 37°C, and virulent or avirulent *C. burnetii* (bacterium-to-cell ratio of 100:1) for 2 h at 37°C. Monocytes were then washed to remove unbound particles. Extracellular E were lyzed by hypotonic shock. Zymosan and E uptake was determined by microscopic examination of cell preparations. Phagocytosis results are expressed as phagocytosis index, which is the product of the number of ingested particles per cell and the percentage of monocytes having ingested at least one particle × 100 (16). The bacterial uptake was determined by immunofluorescence as previously described (5). Monocytes were fixed with 1% paraformaldehyde, and incubated with a 1/250 dilution of rabbit Abs specific for *C. burnetii* in the presence or the absence of 100 μg/ml LPC for 30 min. After washing, cell preparations were incubated with a 1/200 dilution of FITC-conjugated $F(ab')_2$ anti-rabbit IgG. Without LPC, only cell-bound organisms were revealed; bound and ingested organisms were revealed in the presence of LPC. The association index is the product of the number of bacteria per positive cell and the percentage of positive cells × 100. The difference of indexes in the presence and the absence of LPC quantified the uptake of *C. burnetii* (phagocytosis index).

Intracellular fate of C. burnetii

THP-1 monocytes (2×10^5 cells per assay) were pretreated by RANTES (10 ng/ml) for 15 min, incubated with and without mAbs directed against CD18 and CD11b (2.5 μg each), and infected with virulent *C. burnetii* (bacterium-to-cell ratio of 100:1) for 2 h at 37°C. A similar procedure of infection was used with THP-1 cells expressing Nef. Cells were then washed to remove free bacteria; this time was designated as day 0. Infected THP-1 monocytes were cultured in RPMI 1640 containing 20 mM HEPES and 10% heat-inactivated FCS for 4 days. Ingested bacteria were revealed by immunofluorescence as described above. Infection was quantified using an infection index, which is the product of the number of ingested bacteria per cell and the percentage of infected cells × 100. Results are expressed as a relative infection index (compared with values at day 0).

Flow cytometry

THP-1 monocytes (5×10^5 cells per assay) were incubated with mAb directed against CD11b, CD18, $\alpha_v\beta_3$ integrin, IAP, or control IgG1. Cells were then washed and incubated with a 1/50 dilution of FITC-conjugated

$F(ab')_2$ anti-mouse IgG Abs (Immunotech) for 30 min at 4°C. After washing and fixation with 1% paraformaldehyde, cells were analyzed with a FACScan cytometer (BD Biosciences, Le Pont de Claix, France). Monocytes were gated using forward and side scatters, and the fluorescence of 10,000 cells was recorded on the log scale.

Electron microscopy

THP-1 monocytes were fixed in 0.1 M cacodylate buffer (pH 7.2) containing 1% glutaraldehyde for 60 min on a rotating agitator and then incubated overnight in fresh cacodylate solution. After washing, they were incubated in osmium tetroxide for 1 h at 4°C before being dehydrated in acetone and embedded in Epon. Cells were examined with a JEM 1220 JEOL electron microscope (Croissy-sur-Seine, France).

Statistical analysis

Results are given as the mean ± SE and compared with the Mann Whitney *U* test. Some variables are compared with χ^2 test. Differences were considered as significant when $p < 0.05$.

Results

Receptor distribution in C. burnetii*-stimulated monocytes*

THP-1 monocytes were first tagged with mAb directed to monocyte receptors involved in *C. burnetii* recognition, and their distribution was assessed by large beads coated with anti-mouse IgG Abs and F-actin labeling. In resting monocytes, no bead was bound to monocytes tagged with control IgG1 (data not shown). In contrast, beads were attached to monocytes tagged with mAb directed to CD11b, CD18, $\alpha_v\beta_3$ integrin, and IAP (Fig. 1*A*). No bead phagocytosis was observed under our experimental conditions. It is noteworthy that F-actin was peripheral with a moderate concentration underneath attached beads. About 60% of cells tagged with anti-CD11b or anti-CD18 mAb bound beads (1.8 ± 0.5 beads/cell for CD11b and 2.8 ± 0.7 beads/cell for CD18). About 40% of monocytes tagged with mAbs directed against $\alpha_v\beta_3$ integrin or IAP bound beads, and the amounts of beads were slightly lower than those attached to CD11b or CD18 (1.3 ± 0.2 beads/cell for $\alpha_v\beta_3$ integrin and 1.8 ± 0.3 beads/cell for IAP). These results were in agreement with flow cytometry measurements: the expression of $\alpha_v\beta_3$ integrin or IAP on THP-1 monocytes was lower than that of CD11b and CD18 (data not shown). Taken together, these results showed that coated beads are suitable for the investigation of monocyte receptor distribution.

THP-1 monocytes were then stimulated with virulent *C. burnetii* for 15 min, and the distribution of *C. burnetii* receptors was assessed. The stimulation time was chosen as that eliciting pseudopodal extensions and F-actin reorganization (17). Indeed, *C. burnetii* elicited pseudopodal extensions in 60% of THP-1 cells whereas 40% remained undeformed. The distribution of receptors was analyzed in each monocyte subset. In cells without pseudopodal extensions, the distribution of beads attached to CD11b, CD18, $\alpha_v\beta_3$ integrin, and IAP occurred randomly as in control cells (Fig. 1*C*). A distinct pattern was observed in cells with pseudopodal extensions (Fig. 1*B*). All the beads attached to CD11b and CD18 were found outside the deformation area (Table I). The response was observed as early as 10 min after the addition of *C. burnetii*, and CD11b and CD18 remained outside the protrusion until 60 min when *C. burnetii*-stimulated actin reorganization was over (data not shown). In contrast, beads bound to $\alpha_v\beta_3$ integrin were present at the leading edge of the protrusion: one-fourth of beads attached to $\alpha_v\beta_3$ integrin were found in the deformation area (Table I). The pattern of IAP distribution was similar to that of $\alpha_v\beta_3$ integrin, thus emphasizing the previously reported association of $\alpha_v\beta_3$ integrin and IAP (21). The exclusion of CR3 from the protrusions did not result from a lack of sensitivity of the large bead technique. Indeed, when 2.8-μm beads were used instead of 4.5-μm beads, 25% of beads bound to $\alpha_v\beta_3$ integrin and IAP were detected in the pseudopodal extensions, but <10% of beads bound to CD11b and CD18 were found in these extensions (Table I). These results were confirmed by confocal fluorescence microscopy

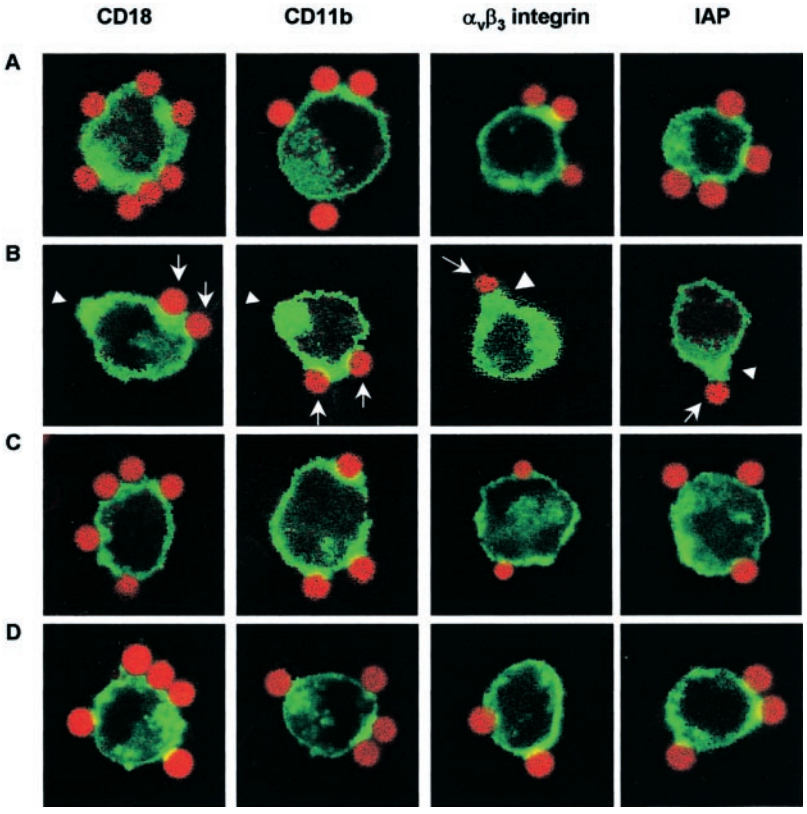

FIGURE 1. Determination of receptor distribution and cytoskeletal organization. THP-1 monocytes (5×10^5 cells/assay) were first stimulated by *C. burnetii* (at a bacterium-to-cell ratio of 100:1) for 15 min, then incubated with specific mAbs, and with beads coated with anti-mouse IgG Abs (5:1 bead-to-cell ratio). F-actin was labeled by 10 U/ml bodipy phallacidin. The colocalization of F-actin and membrane-bound beads was determined with laser scanning confocal microscope. *A*, Control cells. *B*, *C. burnetii*-stimulated cells with pseudopodal extensions; arrowhead, pseudopodal extension; arrow, bead coated with relevant Abs. *C*, *C. burnetii*-stimulated cells without pseudopodal extensions. *D*, Cells stimulated with avirulent *C. burnetii*.

Table I. *Receptor distribution in THP-1 monocytes stimulated by* C. burnetii[a]

	Beads Out of Deformations		Beads in Deformations	
	4.5 μm	2.8 μm	4.5 μm	2.8 μm
CD18	95	109	0 (0%)*	10 (8%)**
CD11b	92	99	0 (0%)*	10 (9%)**
$\alpha_v\beta_3$ integrin	69	84	26 (27%)	27 (24%)
IAP	72	90	24 (25%)	33 (27%)

[a] THP-1 monocytes were incubated with *C. burnetii* (bacterium-to-cell ratio of 100:1) for 15 min at 37°C and the distribution of monocyte receptors was assessed using beads (4.5-μm and 2.8-μm diameter) and F-actin labeling. The number of beads bound to CD18, CD11b, $\alpha_v\beta_3$ integrin, or IAP was determined in and out of the protrusions. The percentage of beads in deformation areas is presented in parentheses.

*, $p < 0.01$ and **, $p < 0.05$ represent the comparison between the distribution of CD18 and CD11b, and that of $\alpha_v\beta_3$ integrin and IAP.

that showed the exclusion of CR3 from the pseudopodal extensions. Indeed, CD11b and CD18 were not detected in the protrusions in 70% of deformed THP-1 monocytes, whereas $\alpha_v\beta_3$ integrin and IAP were present in these protrusions (Fig. 2*A*). In 30% of THP-1 monocytes exhibiting pseudopodal extensions, CD11b and CD18 were detected in the deformation areas but the labeling was faint. Taken together, these results demonstrated that CR3 was dramatically excluded from the protrusions induced by *C. burnetii*.

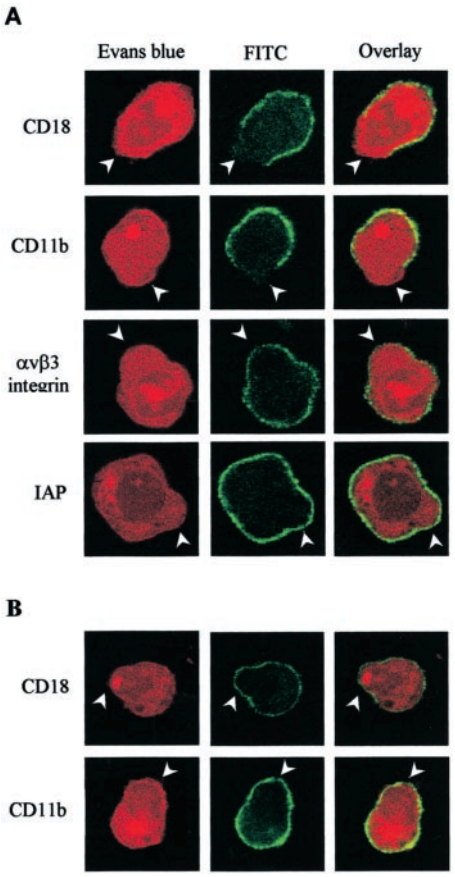

FIGURE 2. Determination of receptor distribution by immunofluorescence. THP-1 monocytes were stimulated by *C. burnetii* (*A*) or RANTES (*B*) for 15 min at 37°C. They were then incubated with specific mAbs, and with FITC-conjugated secondary Abs in the presence of Evans blue. After fixation, cells were observed by confocal microscopy. Evans blue and FITC images were converted into red and green images, and then merged. Arrowheads indicate cell protrusions.

The exclusion of CR3 from the protrusions induced by *C. burnetii* was also observed in circulating monocytes. Monocytes were incubated with 2.8-μm beads, which were suited to the lower size of monocytes. In the deformation areas, only 10% of beads attached to CD11b and CD18 were detected whereas 30% of beads bound to $\alpha_v\beta_3$ integrin and IAP (Table II). The defective redistribution of CR3 toward pseudopodal extensions was specific for the virulent organisms because avirulent variants of *C. burnetii* did not induce pseudopodal extensions and F-actin reorganization and, as a consequence, the distribution of CD11b, CD18, $\alpha_v\beta_3$ integrin, and IAP was similar to control cells (Fig. 1*D*). The defective recruitment of CR3 to cell protrusions did not result from changes in the number of binding sites. The mean number of beads attached to CD11b (1.5 ± 0.3 beads/cell) and CD18 (2.3 ± 0.5 beads/cell) remained similar to that found in the absence of stimulation (see above). The number of beads attached to tagged $\alpha_v\beta_3$ integrin (1.6 ± 0.2 beads/cell) and IAP (1.5 ± 0.3 beads/cell) was similar in control and *C. burnetii*-stimulated THP-1 monocytes. Such findings were confirmed by cytometry experiments that showed the lack of effect of *C. burnetii* on the membrane expression of CR3, $\alpha_v\beta_3$ integrin, and IAP (data not shown and Ref. 5). The exclusion of CR3-bound beads from *C. burnetii*-stimulated protrusions did not depend on the specificity of mAb used. Indeed, THP-1 monocytes were tagged with mAbs directed to distinct domains of CR3, i.e., the lectin-like domain (OKM1) and the I domain (BMS104) of CR3. Beads bound to these mAbs were absent from the pseudopodal extensions (data not shown). Thus, virulent *C. burnetii* organisms, but not avirulent organisms, induce actin-filled pseudopods in human monocytes, and these pseudopodia exclude CR3.

Receptor distribution in RANTES-stimulated monocytes

We wondered whether the defective recruitment of CR3 toward the pseudopodal extensions is specific of *C. burnetii*. When THP-1 monocytes were stimulated with RANTES, a chemokine known to affect the organization of actin cytoskeleton in myeloid cells, a polarized reorganization of F-actin was observed as early as 5 min and peaked at 15 min (Fig. 3*C*, *left panel*). RANTES-induced morphological changes were analyzed by transmission electron microscopy. Monocytes exhibited a polarized broad lamellipodium devoid of intracellular organelles, which was morphologically similar to that elicited by *C. burnetii* (Fig. 3*C*, *right panel*). In contrast to *C. burnetii*-stimulated cells, beads attached to CD11b and CD18 were found in pseudopodal extensions of monocytes stimulated by RANTES (30 and 25%, respectively). The distribution of beads recognizing $\alpha_v\beta_3$ integrin and IAP was similar in cells stimulated by *C. burnetii* and RANTES (27% for $\alpha_v\beta_3$ integrin and 29% for IAP in the deformations induced by RANTES). These results were

Table II. *Receptor distribution in circulating monocytes stimulated by* C. burnetii[a]

	Beads Out of Deformations	Beads in Deformations
CD18	76	8 (10%)*
CD11b	77	10 (11%)*
$\alpha_v\beta_3$ integrin	55	22 (29%)
IAP	57	24 (30%)

[a] Circulating monocytes were incubated with *C. burnetii* (bacterium-to-cell ratio of 100:1) for 15 min at 37°C and the distribution of monocyte receptors was assessed using 2.8-μm beads and F-actin labeling. The number of beads bound to CD18, CD11b, $\alpha_v\beta_3$ integrin, or IAP was determined in and out of the protrusions. The percentage of beads in deformation areas is presented in parentheses.

*, $p < 0.05$ represents the comparison between the distribution of CD18 and CD11b, and that of $\alpha_v\beta_3$ integrin and IAP.

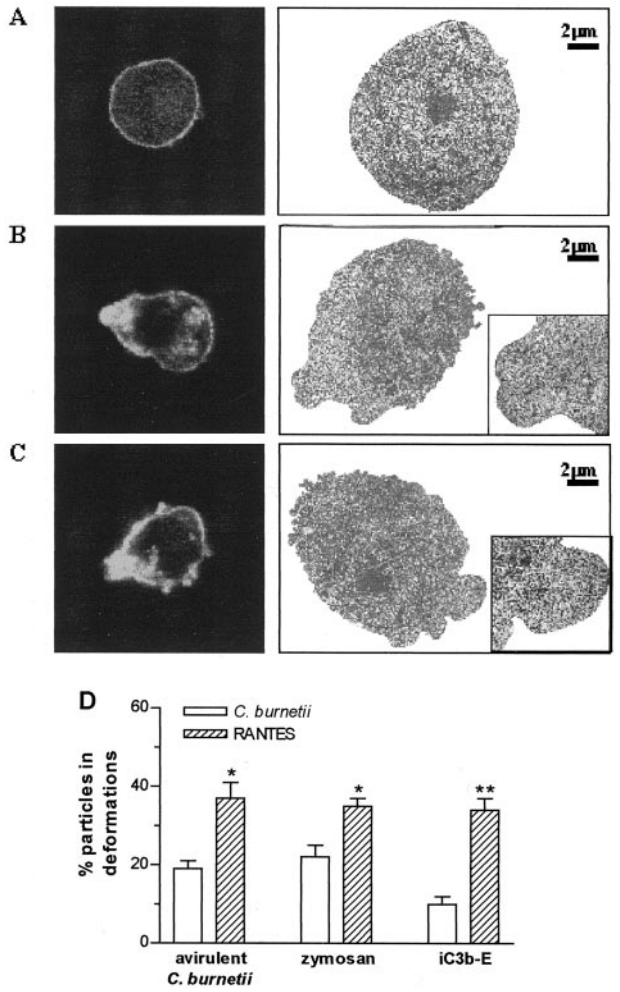

FIGURE 3. Pseudopodal extensions and particle localization. THP-1 monocytes were stimulated by *C. burnetii* (bacterium-to-cell ratio of 100:1) or RANTES (10 ng/ml) for 15 min at 37°C. *A–C*, F-actin was labeled by 10 U/ml bodipy phallacidin, and cells were observed by confocal microscopy (*left*) or by transmission electron microscopy (*right*). Results are representative of three experiments. *A*, Control cells. *B*, Cells stimulated with *C. burnetii*. *C*, Cells stimulated with RANTES. *D*, Stimulated THP-1 monocytes were incubated with avirulent *C. burnetii*, zymosan, or iC3b-coated E for 15 min. Bacteria were detected by immunofluorescence, and zymosan particles and iC3b-coated E by light microscopy. Results are expressed as the percentage of particles present in cell deformations. Results were the mean ± SE of three experiments. *, $p < 0.03$ and **, $p < 0.01$ represent the comparison between pretreatment with *C. burnetii* and RANTES.

confirmed by analysis of CR3 distribution by confocal fluorescence microscopy. Indeed, CD11b and CD18 were present in the pseudopodal extensions induced by RANTES (Fig. 2*B*). Thus, CR3 can enter RANTES-induced pseudopodal extensions in monocytes. This suggests that *C. burnetii* specifically excludes CR3 from pseudopods.

RANTES-mediated restoration of C. burnetii *phagocytosis*

Because RANTES and *C. burnetii* differently affected CR3 redistribution, we studied their effect on binding function of CR3. For that purpose, THP-1 monocytes were pretreated with RANTES or *C. burnetii*, then incubated with particles which need CR3 for optimal binding to monocytes, i.e., iC3b-coated E, zymosan, and avirulent *C. burnetii*. Almost 40% of the particles were associated with pseudopods in RANTES-stimulated monocytes (Fig. 3*D*). In contrast, only 10% of iC3b-coated E ($p < 0.01$) and 20% of avirulent organisms or zymosan particles ($p < 0.03$) were associated with the protrusions in cells pretreated with virulent *C. burnetii*. Hence, the presence of CR3 at the leading edge of the protrusions is associated with increased binding of CR3-dependent particles.

Then, we investigated the effect of RANTES-mediated CR3 redistribution on virulent *C. burnetii* localization, which cannot use CR3 for binding to THP-1 monocytes. In the absence of RANTES treatment, 17 ± 3% of organisms were attached to pseudopodal extensions; this percentage reached 31 ± 6% in cells pretreated with RANTES ($p < 0.05$). Increased *C. burnetii* attachment to pseudopodal extensions results from the availability of CR3. Indeed, virulent organisms were opsonized with iC3b and added to cells pretreated by *C. burnetii* or RANTES. Opsonized organisms were distributed in RANTES-induced pseudopodal extensions whereas they were distributed outside protrusions in *C. burnetii*-stimulated cells (data not shown).

We also investigated the consequences of RANTES-mediated CR3 redistribution on CR3-dependent phagocytosis (Table III). The pretreatment of THP-1 monocytes with virulent *C. burnetii* decreased significantly the phagocytosis of particles and organisms that engage CR3 without opsonization, such as zymosan ($p < 0.05$) and avirulent *C. burnetii* ($p < 0.01$). *C. burnetii* pretreatment of monocytes did not affect the phagocytosis of particles that engage CR3 in an opsonic-dependent manner, such as iC3b-coated E (Table III) or iC3b-coated zymosan (5). In contrast, RANTES did not affect the uptake of particles or organisms that engage CR3 with or without opsonization but RANTES significantly ($p < 0.001$) increased the uptake of virulent organisms, which are normally unable to engage CR3. The RANTES-mediated increase in *C. burnetii* phagocytosis resulted from CR3 engagement. Hence, when a combination of anti-CD11b and anti-CD18 mAbs was added to RANTES-stimulated monocytes, the up-regulation of *C. burnetii* phagocytosis was prevented (phagocytosis index of 110 ± 14 in the absence of anti-CR3 mAb vs 63 ± 7 in the presence of anti-CR3 mAb). Taken together, these results suggest that the increase in *C. burnetii* uptake mediated by RANTES is related to CR3 availability in pseudopodal extensions.

Nef-mediated restoration of C. burnetii *phagocytosis*

As HIV-1 Nef contributes to macrophage activation and modulation of phagocytic receptor expression (18), we wondered whether its expression in THP-1 monocytes interferes with *C. burnetii* phagocytosis as did RANTES stimulation. THP-1 monocytes were transfected with the Nef construct under the control of $CdCl_2$. Hence, Nef was not detected in cells expressing empty vector or

Table III. *Effect of RANTES on particle phagocytosis*[a]

	Pretreatment with		
	None	Virulent *C. burnetii*	RANTES
Virulent *C. burnetii*	60 ± 5	nd	114 ± 8*
Avirulent *C. burnetii*	102 ± 11	55 ± 10**	129 ± 14
Zymosan	94 ± 8	65 ± 9***	119 ± 12
iC3b-coated E	112 ± 21	131 ± 18	95 ± 15
IgG-coated E	128 ± 16	146 ± 12	130 ± 14

[a] THP-1 monocytes were pretreated by *C. burnetii* (bacterium-to-cell ratio of 100:1) or RANTES (10 ng/ml) for 15 min at 37°C, and then incubated with zymosan (1 mg/ml), iC3b-coated E, or IgG-coated E (particle-to-cell ratio of 20:1) for 1 h or *C. burnetii* (bacterium-to-cell ratio of 100:1) for 2 h. Bacteria were detected by immunofluorescence, and zymosan and E by light microscopy. More than 200 monocytes were counted in each assay. Results are expressed as phagocytosis index. They were the mean ± SE of five experiments.

*, $p < 0.001$, **, $p < 0.01$ and ***, $p < 0.05$ represent the comparison between pretreated monocytes and control monocytes. nd = not done.

Nef-transfected cells in the absence of $CdCl_2$, but it was expressed in response to 40 μM $CdCl_2$ in Nef-transfected cells (Fig. 4*A*). The addition of *C. burnetii* to Nef-expressing monocytes elicited the formation of pseudopodal extensions similar to those induced by monocytes that did not express Nef (Fig. 4*B*). We investigated the distribution of CR3 in the protrusions stimulated by *C. burnetii* (Table IV). CD18-bound beads were present in deformation areas of cells that expressed Nef, whereas they were absent from deformation areas of cells that did not express Nef. The distribution of $\alpha_v\beta_3$ integrin was not affected by Nef expression. The overexpression of Nef by THP-1 monocytes up-regulated the uptake of virulent *C. burnetii* (Table V). The increase was similar (2-fold increase) to that induced by RANTES. This increase was dependent on CR3. Indeed, Nef-expressing cells were incubated with *C. burnetii* in the presence of anti-CD11b and anti-CD18 mAb. Control IgG had no effect on *C. burnetii* uptake, whereas CR3-specific mAb decreased *C. burnetii* phagocytosis to the level observed in monocytes that did not express Nef. Thus, Nef expression enables protrusions to redistribute CR3, resulting in the up-regulation of *C. burnetii* phagocytosis.

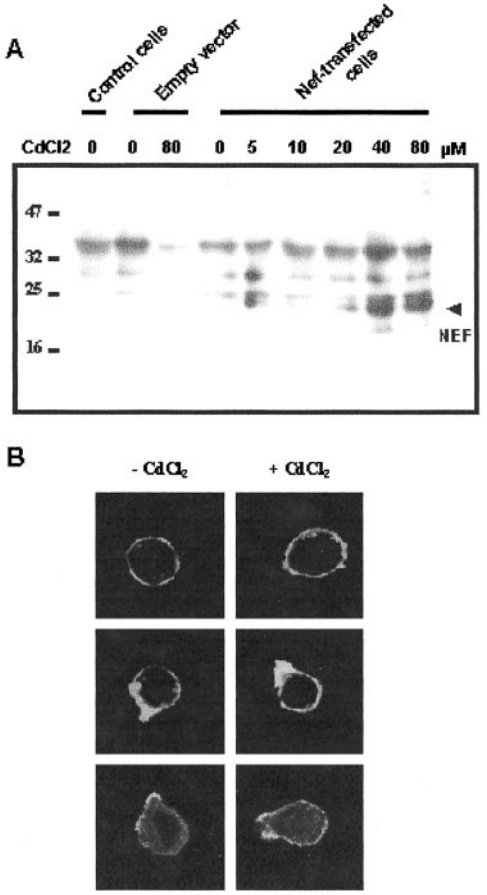

FIGURE 4. Nef expression in monocytes and cytoskeleton reorganization. *A*, THP-1 monocytes with empty vector or Nef construct were incubated in the presence of different concentrations of $CdCl_2$. Nef expression was assessed by SDS-PAGE and immunoblotting with anti-Nef mAb. The blot is representative of three experiments. *B*, Monocytes expressing Nef were stimulated for 15 min. F actin was revealed by 10 U/ml bodipy phallacidin. Results are representative of three experiments. *Top panel*, control cells; *middle panel*, *C. burnetii*-stimulated cells; *bottom panel*, RANTES-stimulated cells.

Table IV. *Effect of Nef expression on the distribution of monocyte receptors*[a]

		Beads Out of Deformations	Beads in Deformations
$-CdCl_2$	CD18	95	0 (0%)*
	$\alpha_v\beta_3$ integrin	69	27 (28%)
$+CdCl_2$	CD18	58	34 (37%)
	$\alpha_v\beta_3$ integrin	72	24 (25%)

[a] Nef-transfected THP-1 monocytes (5×10^5 cells) were incubated with *C. burnetii* (bacterium-to-cell ratio of 100:1) for 15 min at 37°C, and the distribution of CD18 and $\alpha_v\beta_3$ integrin was assessed using beads and F-actin labeling. The number of beads bound to CD18 or $\alpha_v\beta_3$ integrin was determined in and out of the protrusions. In parentheses, the percentage of beads in deformation areas.

*, $p < 0.01$ represents the comparison between monocytes expressing Nef (with 40 μM $CdCl_2$) and those that did not express Nef (without $CdCl_2$).

CR3-dependent phagocytosis and src *kinases*

We recently showed that the activation of Lyn and Hck, two *src* kinases, is associated with the formation of pseudopodal extensions in monocytes stimulated with *C. burnetii* (23). THP-1 monocytes were pretreated with PP1, an inhibitor of *src* kinases (24), and then stimulated by *C. burnetii* or RANTES for 15 min. PP1 did not affect F-actin reorganization induced by RANTES, but it significantly ($p < 0.02$) inhibited the cytoskeleton reorganization stimulated by *C. burnetii* (Table VI). This effect was dose-dependent because it was maximum between 1 and 10 μM PP1 and was lost with 0.01 μM. The effect of PP1 on *C. burnetii* phagocytosis was also studied (Table VI). PP1 up-regulated *C. burnetii* uptake by 150% ($p < 0.05$). In contrast, it did not significantly affect bacterial uptake stimulated by RANTES. The CR3 distribution in cell protrusions could not be studied in PP1-pretreated monocytes stimulated by *C. burnetii* because PP1 prevented the formation of pseudopodal extensions. In RANTES-stimulated monocytes, PP1, which did not prevent the formation of pseudopodal extensions, had no effect on CR3 distribution (~35% of beads were distributed in protrusions vs 25% in control cells). Clearly, *C. burnetii*-mediated cytoskeleton reorganization and CR3 impairment depend on *src* kinases. In contrast, RANTES-mediated up-regulation of *C. burnetii* uptake, cytoskeleton reorganization, and monocyte receptor distribution were independent of PP1-inhibitable *src* kinases.

CR3 distribution and C. burnetii *survival*

As RANTES treatment and Nef expression stimulated CR3 redistribution toward pseudopodal extensions and increased the efficiency of *C. burnetii* phagocytosis, we wondered whether they affected *C. burnetii* survival in THP-1 monocytes. First, cells were pretreated with RANTES for 15 min, infected with virulent organisms for 2 h, and then cultured for 4 days (Fig. 5*A*). In the absence of pretreatment, the infection index increased from days 1 to 3 and thereafter reached a plateau. This survival pattern of *C. burnetii* with low replication is in agreement with our previous results (25).

Table V. *Effect of Nef expression on* C. burnetii *phagocytosis*[a]

	Without $CdCl_2$	With $CdCl_2$
C. burnetii	80 ± 5	170 ± 20*
C. burnetii + anti-CR3 mAb	72 ± 7	96 ± 15

[a] Nef-transfected THP-1 monocytes were incubated with virulent *C. burnetii* (bacterium-to-cell ratio of 100:1) for 2 h in the presence or the absence of anti-CD11b and anti-CD18 mAb (2.5 μg/ml each). *C. burnetii* was detected by immunofluorescence. Results (phagocytosis index) are expressed as mean ± SE of three experiments.

*, $p < 0.002$ represents the comparison between monocytes expressing Nef and those that did not express Nef.

Table VI. *Effect of PP1 on cytoskeleton reorganization and bacterial phagocytosis*[a]

	Pretreatment	
	Without PP1	With PP1
Cytoskeleton reorganization		
None	11 ± 3%	23 ± 5%
C. burnetii	58 ± 8%	24 ± 6%*
RANTES	55 ± 5%	45 ± 8%
C. burnetii phagocytosis		
C. burnetii	51 ± 8	81 ± 9**
RANTES	96 ± 12	82 ± 11

[a] THP-1 monocytes were pretreated with PP1 (10 μM) and then stimulated with virulent *C. burnetii* (bacterium-to-cell ratio of 100:1) or RANTES (10 ng/ml) for 15 min at 37°C. F-actin was labeled by bodipy phallacidin and pseudopodal extensions were analyzed. The results are expressed as the percentage of cells with cell deformations rich in F-actin. For phagocytosis experiments, monocytes were pretreated with PP1, then stimulated with *C. burnetii* or RANTES for 15 min, and *C. burnetii* organisms were added to cells for 2 h. Results are expressed as phagocytosis index. They are the mean ± SE of three experiments.

*, $p < 0.02$ and **, $p < 0.05$ represent the comparison between PP1-pretreated monocytes and control monocytes.

RANTES treatment of THP-1 cells prevented the increase in infection index, which remained constant from days 1 to 4. Second, similar results were obtained with THP-1 monocytes expressing Nef (Fig. 5*B*). In the absence of $CdCl_2$, the infection index was similar to that found in untransfected THP-1 cells. In cells expressing Nef, the infection index remained constant from days 1 to 4 as in RANTES-treated cells. Third, as RANTES and Nef expression may affect *C. burnetii* survival independently of CR3 redistribution, the same experiments were conducted in the presence of anti-CR3 Abs. The uptake of *C. burnetii* was decreased by adding anti-CR3 Abs to RANTES-treated cells and cells expressing Nef (data not shown). Anti-CR3 Abs restored significantly ($p < 0.05$ after 2, 3, and 4 days) *C. burnetii* replication (Fig. 5). These results show that the availability of CR3 impairs *C. burnetii* replication but does not result in bacterial elimination.

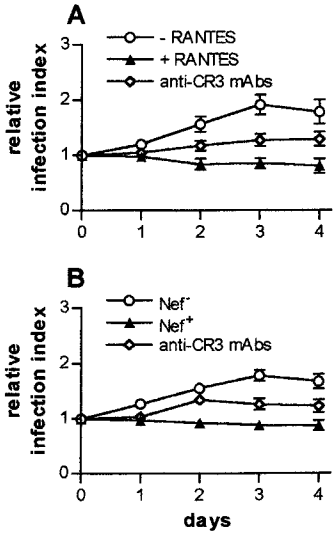

FIGURE 5. Effect of RANTES on the intracellular fate of *C. burnetii*. *A*, THP-1 monocytes were stimulated with RANTES for 15 min, infected by *C. burnetii* in the absence or the presence of anti-CD11b and -CD18 (2.5 μg each) Abs for 2 h and cultured for 4 days. *B*, Nef protein was induced by $CdCl_2$ treatment, and THP-1 monocytes were infected by *C. burnetii* in the absence or presence of anti-CD11b and -CD18 Abs for 2 h and cultured for 4 days. Bacteria were detected by immunofluorescence and the infection index was measured every day. Results are expressed as relative infection index. They were the mean ± SE of three experiments.

Discussion

The phagocytosis of *C. burnetii* is associated with the formation of polarized protrusions (17, 23), the close apposition of the organisms to the protrusions (17), and the impairment of CR3 activity (5). In this study, we report that *C. burnetii* interferes with the redistribution of CR3 toward pseudopodal extensions. The analysis of the relationship between the distribution of monocyte receptors including CR3 and actin cytoskeleton requires a technique visualizing both events. This was achieved by using the method of attaching large beads to surface receptors, which does not affect cytoskeleton organization (20). We compared this method with conventional immunofluorescence. This latter did not allow quantitative analysis of both membrane receptor expression and cytoskeleton because the fluorescence intensity of receptor labeling and cytoskeleton staining were too different. In contrast, conventional immunofluorescence was less dependent of potential steric hindrance due to the size of the beads. Hence, it appears as a complementary method to assess receptor distribution. Using a binding assay of large beads, we showed in this study that CR3 was not detected in pseudopodal extensions stimulated by *C. burnetii*. Similar results were obtained with conventional immunofluorescence. CR3 was absent from the protrusions in most THP-1 cells but faint fluorescence associated with CD11b and CD18 was observed in a minority of cells. This residual presence of CR3 was confirmed using smaller beads. The impaired distribution of CR3 was not the consequence of decreased CR3 expression since the number of CR3-bound beads per cell and the number of CR3 binding sites determined by flow cytometry were not affected by *C. burnetii* stimulation. The distribution of CR3 out of protrusions was specific because other monocyte receptors such as $\alpha_v\beta_3$ integrin, IAP, or CMH class II molecules (data not shown) were distributed randomly on cell surface. The impaired distribution of CR3 was not restricted to THP-1 cells. It was also observed in circulating monocytes which excluded CR3 from the protrusions elicited by *C. burnetii*.

In contrast, chemokine-mediated activation of THP-1 monocytes was associated with cytoskeleton reorganization, but the distribution of CR3 was differently affected. Indeed, RANTES induced polarized protrusions, which exhibited the same morphology and F-actin distribution as *C. burnetii*-stimulated protrusions. However, CR3 was distributed on pseudopodal extensions of RANTES-stimulated monocytes. The selective concentration of receptors in polarized areas of immune cells is in agreement with other reports. Hence, in migrating lymphocytes, $\alpha_v\beta_3$ integrin is concentrated at the leading front, whereas a β_2 integrin such as LFA-1 accumulates at the uropod (26). In T lymphoblasts, RANTES and monocyte chemoattractant protein-1 induce the redistribution of adherence receptors toward the uropod under cytoskeleton control (27). In neutrophils, CR3 is associated with the receptor for the urokinase plasminogen activator and the complex dissociates during polarization: CR3 redistributes toward the uropod while the receptor for urokinase plasminogen activator accumulates at the lamellipodia of migrating neutrophils (28).

The phagocytosis of *C. burnetii* by monocytes is characterized by low efficiency resulting from the impairment of CR3 phagocytic activity (5). The impaired redistribution of CR3 in protrusions may account for altered phagocytic activity of CR3. *C. burnetii* downmodulated the uptake of particles that engage CR3 in a nonopsonic way but had no effect on the phagocytosis of particles that engage CR3 in an opsonic way. RANTES did not affect the uptake of particles that engage CR3. We cannot exclude that other receptors than CR3, such as dectin-1, may promote the phagocytosis of

β-glucan-rich particles such as zymosan in nonopsonic conditions (29, 30). We also reasoned that the availability of CR3 at the leading edge of protrusions improves the probability of physical interaction between CR3 and *C. burnetii*. We clearly showed that RANTES, which promoted CR3 redistribution, increased CR3-mediated binding of *C. burnetii* to pseudopodal extensions and bacterial phagocytosis. Our hypothesis is strengthened by the findings with THP-1 monocytes expressing Nef. The expression of Nef induced the redistribution of CR3 toward pseudopodal extensions and increased CR3-mediated phagocytosis of *C. burnetii*, as did RANTES stimulation of THP-1 monocytes. As basal phagocytosis of *C. burnetii* requires $\alpha_v\beta_3$ integrin and efficient phagocytosis of organisms involves both $\alpha_v\beta_3$ integrin and CR3 (5), it is likely that the redistribution of CR3 improves the functional cross-talk between the two receptors. Indeed, it is well-established that CR3 functions require accessory signals, including that provided by $\alpha_v\beta_3$ integrin (5, 31). In addition, CR3 is able to form membrane complexes with some other receptors (32, 33), which are necessary for its activity.

The mechanisms underlying the impaired distribution of CR3 in cell protrusions did not exclusively result from a mechanical effect of protrusion formation. Indeed, *C. burnetii* and RANTES induced similar cytoskeleton reorganization, but distinct CR3 distribution in cell protrusions. In addition, *C. burnetii* stimulated similar pseudopodal extensions in cells expressing Nef and in control cells, but CR3 was only redistributed in the former. Thus, pseudopod formation and CR3 activity are distinct events, which is in agreement with other reports in which pseudopodal extensions and particle internalization are uncoupled (34). In neutrophils, a chemoattractant such as fMLP induces cell polarization without CR3 aggregation and phagocytosis increase, whereas phorbol esters induce both CR3 aggregation and phagocytosis without cell deformations (9). The mechanisms driving the distribution and the activation of CR3 in cells stimulated by *C. burnetii* or RANTES differently involved *src* kinases. *C. burnetii* stimulates the activation of Lyn and Hck, and their association with the cytoskeleton (23). Their inhibition by PP1, a specific inhibitor of *src* kinases, impaired the formation of cell protrusions and up-regulated bacterial phagocytosis (our results and Ref. 23). But the dramatic effect of PP1 on the cytoskeleton did not allow the assessment of *src* kinases in impaired redistribution of CR3. In RANTES-stimulated cells, PP1 did not affect the formation of pseudopodal extensions, CR3 redistribution, and the up-regulation of *C. burnetii* uptake. Thus, PP1-inhibitable *src* kinases are not involved in RANTES-mediated restoration of CR3-dependent phagocytosis of *C. burnetii*. This finding suggests that other signal molecules than *src* kinases are involved in the effect of RANTES on CR3 distribution and activation. β-chemokines including RANTES have been reported to stimulate the activity of protein tyrosine kinases distinct from *src* kinases such as Pyk2 or Syk (35). Pyk2, a member of the focal adhesion kinase family, has been found in the periphery of the ruffled-leading edge of motile macrophages and to colocalize with CR3 (36), but we have shown that Pyk2 is not activated in *C. burnetii*-stimulated cells (23). β-chemokines induce lateral mobility of LFA-1 and transient increase in its affinity through the activation of phosphatidylinositol 3-kinase (37).

Finally, we wondered whether the redistribution of CR3 and subsequent increased phagocytosis affected the survival of *C. burnetii* in THP-1 monocytes. The role of CR3 in the microbicidal response of monocytes/macrophages is debated and seems to depend on the type of microorganism and the presence of opsonins (31). Hence, organisms such as *Pseudomonas aeruginosa*, *Salmonella* sp., and *Escherichia coli* are eliminated after CR3-mediated uptake whereas others organisms such as *Bordetella* sp. take advantage of CR3 function to avoid bacterial killing (38). The engagement of CR3 by *Mycobacterium tuberculosis* did not affect its intracellular survival (39) and CR3 is not involved in the outcome of *M. tuberculosis* infection (40). The aggregation substance of *Enterococcus faecalis* interacts with CR3, causes increased bacterial uptake, and prevents microbicidal activity of macrophages (41). In this report, whereas *C. burnetii* replicated slowly in control THP-1 monocytes, their treatment with RANTES prevented the replication phase but did not result in bacterial elimination. Similar results were obtained in THP-1 monocytes expressing Nef. The effect of RANTES stimulation and Nef expression on *C. burnetii* replication was inhibited when the engagement of CR3 was prevented with anti-CR3 Abs. This suggests that the control of bacterial replication did not result from specific activation of THP-1 monocytes but was related to CR3 availability. Hence, CR3 may control the replication phase of *C. burnetii*, but the clearance of organisms would require other signals mediated by cytokines such as IFN-γ or TNF (2, 42).

In this report, we showed that the impairment of CR3-mediated phagocytosis of *C. burnetii* is a localized event resulting from altered distribution of CR3 out of pseudopodal extensions. Monocyte activation induced by RANTES or by overexpressing HIV-1 Nef restores both normal distribution of CR3 and *C. burnetii* phagocytosis. The redistribution of CR3 is likely involved in the control of *C. burnetii* replication but could not allow efficient bacterial clearance. Altered localization of phagocytic receptors may represent a strategy of immune escape for intracellular organisms.

Acknowledgments

We thank Derek Mann and Telma Biggs (University of Southampton, U.K.) for providing *nef*-transfected THP-1 monocytes.

References

1. Weisburg, W. G., M. E. Dobson, J. E. Samuel, G. A. Dasch, L. P. Mallavia, O. Baca, L. Mandelco, J. E. Sechrest, E. Weiss, and C. R. Woese. 1989. Phylogenetic diversity of the *Rickettsiae*. *J. Bacteriol. 171:4202.*
2. Ghigo, E., C. Capo, C. H. Tung, D. Raoult, J. P. Gorvel, and J. L. Mege. 2002. *Coxiella burnetii* survival in THP-1 monocytes involves the impairment of phagosome maturation: IFN-γ mediates its restoration and bacterial killing. *J. Immunol. 169:4488.*
3. Mege, J. L., M. Maurin, C. Capo, and D. Raoult. 1997. *Coxiella burnetii*: the "query" fever bacterium: a model of immune subversion by a strictly intracellular microorganism. *FEMS Microbiol. Rev. 19:209.*
4. Maurin, M., and D. Raoult. 1999. Q fever. *Clin. Microbiol. Rev. 12:518.*
5. Capo, C., F. P. Lindberg, S. Meconi, Y. Zaffran, G. Tardei, E. J. Brown, D. Raoult, and J. L. Mege. 1999. Subversion of monocyte functions by *Coxiella burnetii*: impairment of the cross-talk between $\alpha_v\beta_3$ integrin and CR3. *J. Immunol. 163:6078.*
6. Hynes, R. O. 1992. Integrins: versatility, modulation, and signaling in cell adhesion. *Cell 69:11.*
7. Van Strijp, J. A., D. G. Russell, E. Tuomanen, E. J. Brown, and S. D. Wright. 1993. Ligand specificity of purified complement receptor type three (CD11b/CD18, $\alpha_M\beta_2$, Mac-1). Indirect effects of an Arg-Gly-Asp (RGD) sequence. *J. Immunol. 151:3324.*
8. Ishibashi, Y., S. Claus, and D. A. Relman. 1994. *Bordetella pertussis* filamentous hemagglutinin interacts with a leukocyte signal transduction complex and stimulates bacterial adherence to monocyte CR3 (CD11b/CD18). *J. Exp. Med. 180: 1225.*
9. Detmers, P. A., S. D. Wright, E. Olsen, B. Kimball, and Z. A. Cohn. 1987. Aggregation of complement receptors on human neutrophils in the absence of ligand. *J. Cell Biol. 105:1137.*
10. Schwartz, M. A., M. D. Schaller, and M. H. Ginsberg. 1995. Integrins: emerging paradigms of signal transduction. *Annu. Rev. Cell. Dev. Biol. 11:549.*
11. Pavalko, F. M., and S. M. LaRoche. 1993. Activation of human neutrophils induces an interaction between the integrin β_2-subunit (CD18) and the actin binding protein α-actinin. *J. Immunol. 151:3795.*
12. Sharma, C. P., R. M. Ezzell, and M. A. Arnaout. 1995. Direct interaction of filamin (ABP-280) with the β_2-integrin subunit CD18. *J. Immunol. 154:3461.*
13. Graham, I. L., H. D. Gresham, and E. J. Brown. 1989. An immobile subset of plasma membrane CD11b/CD18 (Mac-1) is involved in phagocytosis of targets recognized by multiple receptors. *J. Immunol. 142:2352.*
14. Kucik, D. F., M. L. Dustin, J. M. Miller, and E. J. Brown. 1996. Adhesion-activating phorbol ester increases the mobility of leukocyte integrin LFA-1 in cultured lymphocytes. *J. Clin. Invest. 97:2139.*
15. Zhou, B., J. A. Weigel, L. Fauss, and P. H. Weigel. 2000. Identification of the hyaluronan receptor for endocytosis (HARE). *J. Biol. Chem. 275:37733.*

16. Capo, C., S. Meconi, M. V. Sanguedolce, N. Bardin, G. Flatau, P. Boquet, and J. L. Mege. 1998. Effect of cytotoxic necrotizing factor-1 on actin cytoskeleton in human monocytes: role in the regulation of integrin-dependent phagocytosis. *J. Immunol. 161:4301.*
17. Meconi, S., V. Jacomo, P. Boquet, D. Raoult, J. L. Mege, and C. Capo. 1998. *Coxiella burnetii* induces reorganization of the actin cytoskeleton in human monocytes. *Infect. Immun. 66:5527.*
18. Biggs, T. E., S. J. Cooke, C. H. Barton, M. P. Harris, K. Saksela, and D. A. Mann. 1999. Induction of activator protein 1 (AP-1) in macrophages by human immunodeficiency virus type-1 Nef is a cell-type-specific response that requires both *hck* and MAPK signaling events. *J. Mol. Biol. 290:21.*
19. Collette, Y., H. Dutartre, A. Benziane, M. Ramos, R. Benarous, M. Harris, and D. Olive. 1996. Physical and functional interaction of Nef with Lck: HIV-1 Nef-induced T-cell signaling defects. *J. Biol. Chem. 271:6333.*
20. Wulfing, C., and M. M. Davis. 1998. A receptor/cytoskeletal movement triggered by costimulation during T cell activation. *Science 282:2266.*
21. Brown, E., L. Hooper, T. Ho, and H. Gresham. 1990. Integrin-associated protein: a 50-kD plasma membrane antigen physically and functionally associated with integrins. *J. Cell Biol. 111:2785.*
22. Lindberg, F. P., D. C. Bullard, T. E. Caver, H. D. Gresham, A. L. Beaudet, and E. J. Brown. 1996. Decreased resistance to bacterial infection and granulocyte defects in IAP-deficient mice. *Science 274:795.*
23. Meconi, S., C. Capo, M. Remacle-Bonnet, G. Pommier, D. Raoult, and J. L. Mege. 2001. Activation of protein tyrosine kinases by *Coxiella burnetii*: role in actin cytoskeleton reorganization and bacterial phagocytosis. *Infect. Immun. 69:2520.*
24. Liu, Y., A. Bishop, L. Witucki, B. Kraybill, E. Shimizu, J. Tsien, J. Ubersax, J. Blethrow, D. O. Morgan, and K. M. Shokat. 1999. Structural basis for selective inhibition of Src family kinases by PP1. *Chem. Biol. 6:671.*
25. Dellacasagrande, J., C. Capo, D. Raoult, and J. L. Mege. 1999. IFN-γ-mediated control of *Coxiella burnetii* survival in monocytes: the role of cell apoptosis and TNF. *J. Immunol. 162:2259.*
26. Sanchez-Madrid, F., and M. A. del Pozo. 1999. Leukocyte polarization in cell migration and immune interactions. *EMBO J. 18:501.*
27. del Pozo, M. A., P. Sanchez-Mateos, M. Nieto, and F. Sanchez-Madrid. 1995. Chemokines regulate cellular polarization and adhesion receptor redistribution during lymphocyte interaction with endothelium and extracellular matrix: involvement of cAMP signaling pathway. *J. Cell Biol. 131:495.*
28. Kindzelskii, A. L., Z. O. Laska, R. F. Todd, and H. R. Petty. 1996. Urokinase-type plasminogen activator receptor reversibly dissociates from complement receptor type 3 ($\alpha_M\beta_2$, CD11b/CD18) during neutrophil polarization. *J. Immunol. 156:297.*
29. Brown, G. D., and S. Gordon. 2001. Immune recognition: a new receptor for β-glucans. *Nature 413:36.*
30. Taylor, P. R., G. D. Brown, D. M. Reid, J. A. Willment, L. Martinez-Pomares, S. Gordon, and S. Y. Wong. 2002. The β-glucan receptor, dectin-1, is predominantly expressed on the surface of cells of the monocyte/macrophage and neutrophil lineages. *J. Immunol. 169:3876.*
31. Underhill, D. M., and A. Ozinsky. 2002. Phagocytosis of microbes: complexity in action. *Annu. Rev. Immunol. 20:825.*
32. May, A. E., S. M. Kanse, L. R. Lund, R. H. Gisler, B. A. Imhof, and K. T. Preissner. 1998. Urokinase receptor (CD87) regulates leukocyte recruitment via β_2 integrins in vivo. *J. Exp. Med. 188:1029.*
33. Xia, Y., G. Borland, J. Huang, I. F. Mizukami, H. R. Petty, R. F. Todd, and G. D. Ross. 2002. Function of the lectin domain of Mac-1/complement receptor type 3 (CD11b/CD18) in regulating neutrophil adhesion. *J. Immunol. 169:6417.*
34. Lowry, M. B., A. M. Duchemin, J. M. Robinson, and C. L. Anderson. 1998. Functional separation of pseudopod extension and particle internalization during Fcγ receptor-mediated phagocytosis. *J. Exp. Med. 187:161.*
35. Dikic, I., and J. Schlessinger. 1998. Identification of a new Pyk2 isoform implicated in chemokine and antigen receptor signaling. *J. Biol. Chem. 273:14301.*
36. Duong, L. T., and G. A. Rodan. 2000. PYK2 is an adhesion kinase in macrophages, localized in podosomes and activated by β_2-integrin ligation. *Cell Motil. Cytoskeleton 47:174.*
37. Constantin, G., M. Majeed, C. Giagulli, L. Piccio, J. Y. Kim, E. C. Butcher, and C. Laudanna. 2000. Chemokines trigger immediate β_2 integrin affinity and mobility changes: differential regulation and roles in lymphocyte arrest under flow. *Immunity 13:759.*
38. Agramonte-Hevia, J., A. Gonzalez-Arenas, D. Barrera, and M. Velasco-Velazquez. 2002. Gram-negative bacteria and phagocytic cell interaction mediated by complement receptor 3. *FEMS Immunol. Med. Microbiol. 34:255.*
39. Hirsch, C. S., J. J. Ellner, D. G. Russell, and E. A. Rich. 1994. Complement receptor-mediated uptake and tumor necrosis factor-α-mediated growth inhibition of *Mycobacterium tuberculosis* by human alveolar macrophages. *J. Immunol. 152:743.*
40. Hu, C., T. Mayadas-Norton, K. Tanaka, J. Chan, and P. Salgame. 2000. *Mycobacterium tuberculosis* infection in complement receptor 3-deficient mice. *J. Immunol. 165:2596.*
41. Sussmuth, S. D., A. Muscholl-Silberhorn, R. Wirth, M. Susa, R. Marre, and E. Rozdzinski. 2000. Aggregation substance promotes adherence, phagocytosis, and intracellular survival of *Enterococcus faecalis* within human macrophages and suppresses respiratory burst. *Infect. Immun. 68:4900.*
42. Dellacasagrande, J., E. Ghigo, D. Raoult, C. Capo, and J. L. Mege. 2002. IFN-γ-induced apoptosis and microbicidal activity in monocytes harboring the intracellular bacterium *Coxiella burnetii* require membrane TNF and homotypic cell adherence. *J. Immunol. 169:6309.*